Available online at www.sciencedirect.com
SCIENCE DIRECT®
ELSEVIER
Journal of the European Ceramic Society 25 (2005) 2369–2372
ECRS
www.elsevier.com/locate/jeurceramsoc

Polarization profiling of metal-ferroelectric-semiconductor structures by LIMM

G. Suchaneck[a,*], A.V. Solnyshkin[b], A. Suchaneck[a], G. Gerlach[a]

[a] *Technische Universität Dresden, Institut für Festkörperelektronik, Helmholtzstrasse 10, 01062 Dresden, Germany*
[b] *Tver State University, Department of Ferroelectric and Piezoelectric Physics, Sadovij per. 35, 170002 Tver, Russia*

Available online 23 March 2005

Abstract

In this work, the laser intensity modulation method (LIMM) is applied for the investigation of metal-ferroelectric-semiconductor structures. In particular, Pt/ferroelectric PZT (perovskite)/semi-conducting PZT (fluorite) was investigated. The pyroelectric coefficient profile was reconstructed using an simplified analytic solution of the LIMM problem and a thermal model consisting of up to eight different layers. Thermal expansion in (1 1 1) direction was calculated from the *a*-axis and *c*-axis values. The temperature coefficient of the dielectric constant was determined in the saturation range of the P–E hysteresis at various temperatures between 0 and 60 °C: (i) for the as deposited self-polarized films; (ii) from the slope of the hysteresis in the saturation range of the ferroelectric hysteresis; from (iii) from capacitance measurements of biased samples in the saturation range of the ferroelectric hysteresis.
© 2005 Elsevier Ltd. All rights reserved.

Keywords: Ferroelectric properties; PZT; Perovskites; Pyroelectric spectroscopy

1. Introduction

The polarization of ferroelectric films sandwiched between metal and semiconducting electrodes was investigated for more than 30 years. However, there is yet no demonstrative experimental determination of the polarization depth profile in such a multilayer structure.

Recently, the laser intensity modulation method (LIMM), e.g., the determination of the spatial polarization profile from the current-response spectrum caused by the interaction of thermal waves generated by an intensity modulated laser and the unknown polarization profile, was applied to the investigation of ferroelectric thin films.[1] In order to study thin films with a thickness of about 1 μm, both the modulation frequency of the laser was extended into the MHz range and the multilayer structure of thin film sensors was included into the thermal model. For solving the "ill-posed" LIMM problem, the profile reconstruction was performed by using algorithms for the inverse solution of the appropriate FREDHOLM integral equation and a TIKHONOV regularization method for stable numerical solutions. By this technique, smooth profiles were reconstructed using an appropriate thermal multilayer model within an uncertainty of 2–3% in dependence on the discretization approach. On the other hand, the uncertainty of the reconstruction of a Dirac-pulse-like polarization profile exceeds 90%.[2] Therefore, the reconstruction of profiles with discontinuities, for instance at interfaces, using numerical algorithms is not satisfactory.

In this work, LIMM is applied for investigation of a metal-ferroelectric-semiconductor structure, particularly Pt/ferroelectric PZT (perovskite)/semiconducting PZT (fluorite). The pyroelectric coefficient profile was reconstructed using an simplified analytic solution of the LIMM problem and a thermal model consisting of up to eight different layers.

2. Theory

We consider a ferroelectric-semiconductor heterojunction where the ferroelectric material shows no interface states and where the interface is characterized by a gaussian space charge distribution. In this case, the distribution of the

* Corresponding author. Tel.: +49 351 463 5281; fax: +49 351 463 2320.
E-mail address: suchanec@rcs.urz.tu-dresden.de (G. Suchaneck).

0955-2219/$ – see front matter © 2005 Elsevier Ltd. All rights reserved.
doi:10.1016/j.jeurceramsoc.2005.03.058

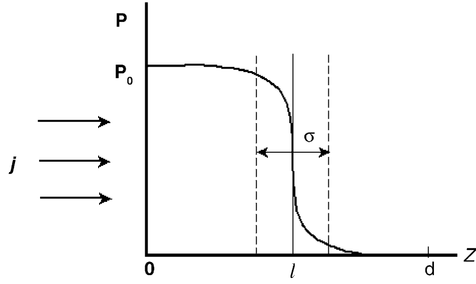

Fig. 1. Approximate polarization distribution near a ferroelectric-semiconductor interface.

pyroelectric coefficient is given by[3]:

$$p(z) = p_0\left(1 - \frac{1}{\sigma\sqrt{\pi}}\int_0^z \exp\left\{-\left(\frac{z'-l}{\sigma}\right)^2\right\}\mathrm{d}z'\right) = \frac{p_0}{2}\left[1 - \mathrm{erf}\left(\frac{z-l}{\sigma}\right)\right], \quad (1)$$

where p_0 is the pyroelectric coefficient in the bulk of the film, σ defines the polarization decay ($3\sigma < l$, where l is ferroelectric thickness), erf is the integral of the Gauss distribution (the error function), and z is the film depth (Fig. 1).

The depth profile of the pyroelectric coefficient $p(z)$ may be determined from the pyroelectric current spectrum $I(\omega, t)$ caused by the propagation of a thermal wave through the ferroelectric film. If the heating is produced by sinusoidally modulated laser light with circular frequency ω, the complex pyroelectric current yields[4]:

$$I(\omega, t) = I\ \exp\{\mathrm{i}\omega t\} = \frac{A}{d}\int_0^d \frac{p_0}{2}\left[1 - \mathrm{erf}\left(\frac{z-l}{\sigma}\right)\right]\frac{\partial T(z,\ \omega,\ t)}{\partial t}\,\mathrm{d}z, \quad (2)$$

where $I_\sim$ is the complex amplitude of the pyroelectric current, t the time, T the temperature distribution inside the sample, A the heated area of the sample, and d the total thickness of the ferroelectric and the semiconductor layers. Eq. (2) can be easily integrated numerically. The numerical reconstruction of the pyroelectric coefficient profile is based on a thermal model consisting of up to eight layers (air-top electrode-PZT-bottom electrode-adhesion layer Si_3N_4–SiO_2–Si).[5]

An analytical solution of Eq. (2) exists only for the single layer case. Assuming that the thermal properties of the ferroelectric and the semiconductor films are approximately the same, we obtain the well known solution for the pyroelectric current in the case of a one-dimensional heat conduction problem of a thermally insulated single layer[5]:

$$I_\sim = \frac{Aj_\sim\eta}{\mathrm{d}c\rho}\frac{k}{\sinh(kd)}\int_0^d p(z)\cosh[k(d-z)]\,\mathrm{d}z = C\int_0^d p(z)\cosh[k(d-z)]\,\mathrm{d}z, \quad (3)$$

where $j_\sim$ is the amplitude of the laser beam intensity, η the absorbance of the irradiated surface, c the heat capacity, ρ the mass density, k the complex wavenumber:

$$k = (1+i)\sqrt{\frac{\omega}{2D}}, \quad (4)$$

and D the thermal diffusivity. Inserting Eq. (2) into Eq. (3), we find:

$$I_\sim = C\frac{p_0}{2}\int_0^d\left[\left(1-\mathrm{erf}\left\{\frac{z-l}{\sigma}\right\}\right)\cosh\{k(d-z)\}\right]\mathrm{d}z = C\frac{p_0}{2}\frac{\sinh(kd)}{k} - C\frac{p_0}{2}\int_0^d\left[\mathrm{erf}\left\{\frac{z-l}{\sigma}\right\}\cosh\{k(d-z)\}\right]\mathrm{d}z. \quad (5)$$

Representing the erf function as a series[3]:

$$\mathrm{erf}\left\{\frac{z-l}{\sigma}\right\} = \frac{2}{\sqrt{\pi}}\sum_{n=0}^{\infty}\frac{(-1)^n(z-l/\sigma)^{2n+1}}{n!(2n+1)}, \quad (6)$$

Eq. (5) can be integrated. The complex pyroelectric current becomes:

$$I_\sim = C\frac{p_0}{2}\frac{\sinh(kd)}{k} - C\frac{p_0}{2}\frac{2}{\sqrt{\pi}}\int_0^d\sum_{n=0}^{\infty}\frac{(-1)^n(z-l/\sigma)^{2n+1}}{n!\,(2n+1)} \times \cosh[k(d-z)]\,\mathrm{d}z = C\frac{p_0}{2}\left\{\frac{\sinh(kd)}{k} - \frac{2}{\sqrt{\pi}}\sum_{n=0}^{\infty} \times \frac{(-1)^n}{n!(2n+1)}\int_0^d\left(\frac{z-l}{\sigma}\right)^{2n+1}\cosh[k(d-z)]\,\mathrm{d}z\right\}, \quad (7)$$

and the final analytical solution is:

$$I_\sim = \frac{Aj_\sim\eta}{\mathrm{d}c\rho}\frac{p_0}{2} - \frac{Aj_\sim\eta}{\mathrm{d}c\rho}\frac{p_0}{\sqrt{\pi}}\sum_{n=0}^{\infty}\left[\frac{(-1)^n 2^n}{(\sigma k)^{2(n+1)}} \times \sum_{p=0}^{2n+1}\frac{(kl)^p\cosh(kd) - (k(d-l))^p}{p!}\right] \quad (8)$$

A similar calculation can be made for the case of a thermally coupled single layer where[5]:

$$I_\sim = \frac{Aj_\sim\eta}{\mathrm{d}c\rho}\frac{k}{\cosh(kd)}\int_0^d p(z)\sinh[k(d-z)]\,\mathrm{d}z = C\int_0^d p(z)\sinh[k(d-z)]\,\mathrm{d}z. \quad (9)$$

3. Comparison with experiment

In general, the temperature change causes thermal expansion and the dielectric constant depends on temperature. Therefore, the pyroelectric response function becomes[4]:

$$r(z) = p(z) - (\alpha_z - \alpha_\varepsilon)\varepsilon\varepsilon_0 E_{\text{int}}(z). \quad (10)$$

Here, $p(z)$ is the pyroelectric coefficient, α_z the relative thermal expansion coefficient, α_ε the relative temperature coefficient of the dielectric constant, ε the dielectric constant, and E_{int} the internal electric field.

The thermal expansion coefficient of (1 1 1) oriented PZT 30/70 films was derived from the temperature dependence of the lattice parameters c and a from room temperature up to the Curie temperature.[6] This results in $\alpha_a = \alpha_1 = \alpha_2 = 2.5 \times 10^{-5}\,\text{K}^{-1}$ and $\alpha_c = \alpha_3 = -4.8 \times 10^{-5}\,\text{K}^{-1}$. A coordinate transformation to a z-axis along [1 1 1] gives:

$$\alpha_z = \alpha'_3 = \frac{\alpha_1 + \alpha_2 - \alpha_3}{3} \approx 7 \times 10^{-7}\,\text{K}^{-1}. \quad (11)$$

Note, that we have not considered the different orientation of the grains in the X–Y plane. Taking into account that the electric field in the space charge layer cannot exceed the coercive field in order of 10^7 V/m, the term consisting α_z in Eq. (10) can be neglected.

The relative temperature coefficient α_r of the dielectric constant was determined: (i) from capacitance measurements of the as deposited self-polarized PZT thin film (point 1 in Fig. 2); (ii) capacitance measurements of biased samples in the saturation range of the P–E hysteresis (point 2 in Fig. 2); and (iii) the slope of the P–E hysteresis in the saturation range (point 3 in Fig. 2).

Fig. 3 illustrates that in all cases the dielectric response is dominated by the ferroelectric part dP/dE. For LIMM analysis we used the small signal values $\alpha_\varepsilon = 1.5 \times 10^{-3}$ of the self-polarized PZT films which are frequency-independent at least up to 100 kHz. Taking an internal electric field close to the coercive field of the self-polarized state of about 1×10^5 V/cm, the second term of Eq. (10) yields to less than 5 nC/cm^2 K, i.e. to less than 25% of the bulk pyrocoefficient value.

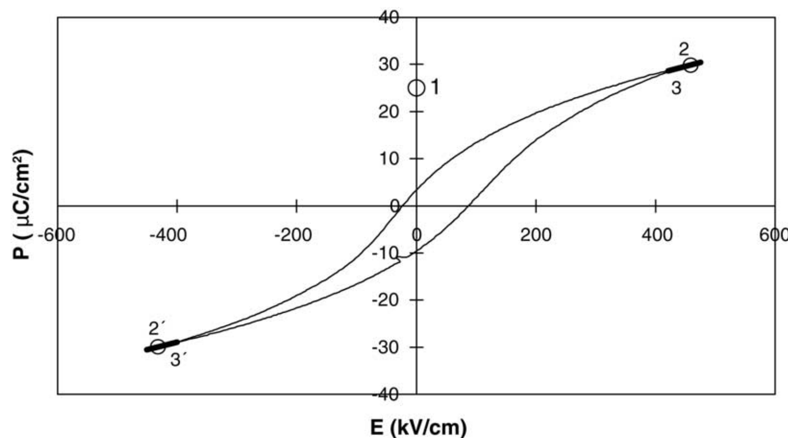

Fig. 2. P–E hysteresis loop of a perovskite PZT thin film with a thickness of 900 nm. The dielectric constant was determined in the marked points.

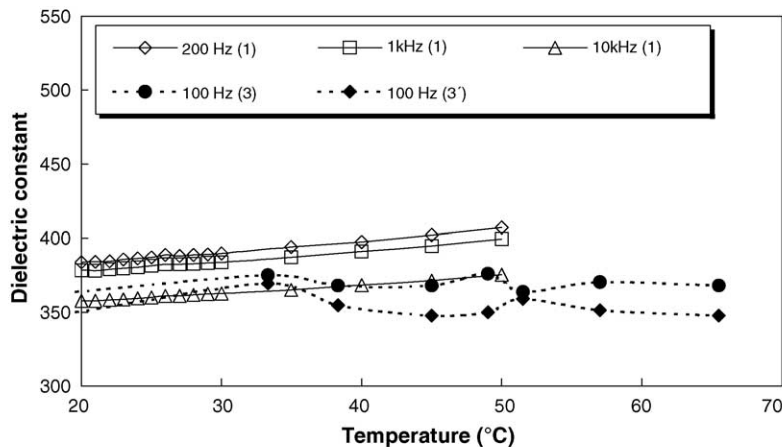

Fig. 3. Comparison of the temperature dependence of the dielectric constant obtained from capacitance measurements of the as deposited self-polarized PZT film (1), and the slope of the P–E hysteresis (3).

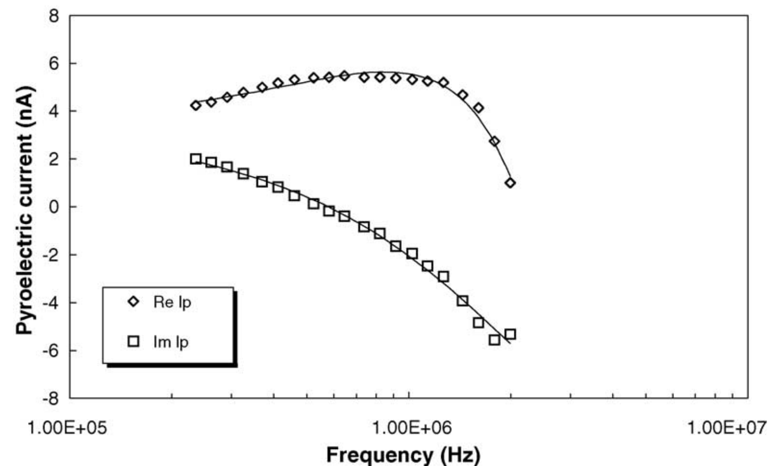

Fig. 4. Pyroelectric current spectrum of a 300 nm perovskite PZT/400 nm fluorite PZT structure in comparison with the spectrum obtained from Eq. (2) ($\sigma/l = 0.18$).

Therefore, in a first approximation the second term of Eq. (10) may be neglected.

The effective piezocoefficient d_{33}^* was derived from the initial slope of the piezoelectric vibration amplitude plotted versus the amplitude of the applied to the cantilever AC voltage. Here, values of 9 and 16 pm/V are in good agreement with other measurements of (1 1 1) textured PZT thin films.[7,8] They give evidence that secondary piezoelectric effects in z-direction can be neglected.

Fig. 4 illustrates the fit of Eq. (2) to the pyroelectric spectrum of a 300 nm perovskite PZT/400 nm fluorite PZT structure. A satisfactory conformance was obtained only when the thermal load of the substrate was taken into account. Thus the effective thermal diffusivity seen by the ferroelectric layer is significantly lower than expected from Eq. (8).

4. Conclusions

An approximate polarization distribution of the ferroelectric PZT thin film structure including a ferroelectric-semiconductor interface with a PZT fluorite phase as semiconductor was determined considering a simplified problem of a gaussian space charge distribution at the interface without interface states. However, even in this simplified case, the specimen multilayer structure must be taken into account in the thermal model.

Acknowledgements

This work was supported by the German Research Council (Deutsche Forschungsgemeinschaft) as part of the Research Group FOR520 and by the Herbert Quandt Foundation. The authors thank F. Schlaphof (Dresden University of Technology, Institute for Applied Photophysics) for the determination of the piezoelectric coefficient and T. Sandner for the measurement of the pyroelectric current spectrum.

References

1. Sandner, T., Suchaneck, G., Koehler, R., Suchaneck, A. and Gerlach, G., High frequency LIMM—a powerful tool for ferroelectric thin film characterization. *Integr. Ferroelectr.*, 2002, **46**, 243–257.
2. Gerlach, G., Sandner, T. and Suchaneck, G., Determination of polarization profiles inside ferroelectric thin films using the laser intensity modulation method. In *Testing, Reliability, and Application of Micro- and Nano-Material Systems, Proceedings of SPIE, Vol 5045*, ed. N. Meyendorf, G. Y. Baaklini and B. Michel. SPIE, Bellingham, 2003, pp. 157–171.
3. *Handbook of Mathematical Functions with Formulas, Graphs and Mathematical Tables*, ed. M. Abramowitz and I. R. Stegun. Applied Mathematics Series 53, National Bureau of Standards, Washington, 1964.
4. Ploss, B., Emmerich, R. and Bauer, S., Thermal wave probing of pyroelectric distributions in the surface region of ferroelectric materials: a new methode of analysis. *J. Appl. Phys.*, 1992, **72**, 5363–5370.
5. Sandner, T., Gerlach, G., Suchaneck, G. and Koehler, R., Depth resolved polarization profiles in pyroelectric thin films (in German). *Technisches Messen*, 1999, **66**, 322–332.
6. Bruchhaus, R., Pitzer, D., Primig, R., Wersing, W. and Xu, Y., Deposition of self-polarized PZT films by planar multi-target sputtering. *Integr. Ferroelectr.*, 1997, **14**, 141–149.
7. Lian, L. and Sottos, N. R., Effects of thickness on the piezoelectric and dielectric properties of lead zirconate titanate thin films. *J. Appl. Phys.*, 2000, **87**, 3941–3949.
8. Kholkin, A., Electromechanical properties of ferroelectric films for MEMS. *Ferroelectrics*, 2001, **258**, 209–220.